Energetic proton acceleration associated with Io's footprint tail

G. Clark[1], B. H. Mauk[1], P. Kollmann[1], J. R. Szalay[2], A. H. Sulaiman[3], D. J. Gershman[4], J. Saur[5], S. Janser[5], K. Garcia-Sage[4], T. Greathouse[6], C. Paranicas[1], F. Allegrini[6,7], F. Bagenal[8], S. J. Bolton[6], J. E. P. Connerney[9,4], R.W. Ebert[6,7], G. Hospodarsky[3], D. Haggerty[1], V. Hue[6], M. Imai[10], S. Kotsiaros[11], D. J. McComas[2], A. Rymer[1], J. Westlake[1]

[1]Johns Hopkins University Applied Physics Laboratory, Laurel, MD

[2] Department of Astrophysical Sciences, Princeton University, Princeton, New Jersey

[3] Department of Physics and Astronomy, University of Iowa, Iowa City, IA

[4] NASA Goddard Space Flight Center, Greenbelt, MD

[5] University of Cologne, Cologne, Germany

[6] Southwest Research Institute, San Antonio, TX

[7] University of Texas at San Antonio, San Antonio, TX

[8] Laboratory for Atmospheric and Space Physics, University of Colorado, Boulder, CO

[9] Space Research Corporation, Annapolis, MD

[10] Department of Electrical Engineering and Information Science, National Institute of Technology (KOSEN), Niihama College, Niihama, Japan

[11] National Space Institute Measurement and Instrumentation Systems, DTU, Denmark

Corresponding author: George Clark (george.clark@jhuapl.edu)

Key Points:

- Juno's likely crossing of Io's Main Alfvén Wing (MAW) during PJ12 reveals evidence of transverse ion acceleration
- Observations suggest wave-particle interactions with ion cyclotron waves as the favored acceleration mechanism; however, Alfvén acceleration was not ruled out.
- Ion conics generated in Io's footprint tail or near the MAW are more intense and energetic than observed in other auroral regions

Abstract

Observations of energetic charged particles associated with Io's footprint (IFP) tail, and likely within or very near the Main Alfvén Wing, during Juno's 12th perijove (PJ) crossing show evidence of intense proton acceleration by wave-particle heating. Measurements made by Juno/JEDI reveal proton characteristics that include pitch angle distributions concentrated along the upward loss cone, broad energy distributions that span ~50 keV to 1 MeV, highly structured temporal/spatial variations in the particle intensities, and energy fluxes as high as ~100 mW/m^2. Simultaneous measurements of the plasma waves and magnetic field suggest the presence of ion cyclotron waves and transverse Alfvénic fluctuations. We interpret the proton observations as upgoing conics likely accelerated via resonant interactions with ion cyclotron waves. These observations represent the first measurements of ion conics associated with moon-magnetosphere interactions, suggesting energetic ion acceleration plays a more important role in the IFP tail region than previously considered.

Plain-Language Summary

NASA's Juno spacecraft orbits Jupiter's polar region and makes direct measurements of the fields and particles that are responsible for creating Jupiter's powerful auroras. In this article, we present new observations that show intense proton acceleration occurring at altitudes near the auroral emissions created by the interaction between Jupiter's moon Io and the surrounding plasma and magnetic field environment. These unique observations provide clues on how particles are being accelerated and will help constrain particle acceleration theories.

1. Introduction

Juno's exploration of Jupiter's polar magnetosphere (Bagenal et al., 2017, Connerney et al., 2017a) has given prominence to the "far-field" region of the Io-Jupiter interaction with new *in situ* measurements of Io's footprint (IFP) tail auroral emissions. The far-field interaction specifically refers to the electromagnetic coupling between Io and Jupiter's ionosphere. Decades of remote observations have established that Io generates steady auroral emissions in the radio (Bigg et al., 1964, Queinnec and Zarka, 1998, Zarka 2000), infrared (Connerney et al. 1993), and ultraviolet wavelengths (Clarke et al., 1996). Furthermore, more recent HST observations and analyses have characterized its auroral structuring (Bonfond et al. 2008) and correlated brightness changes with Io's centrifugal latitude (Gérard et al. 2006). Previous flybys of Io from the Voyager and Galileo missions mapped out the local Io-plasma interaction. Plasma and energetic particle (e.g., Belcher et al. 1981, Frank et al. 1996, Williams et al. 1996, Gurnett et al. 1996) and magnetic field (e.g., Acuña et al. 1981, Kivelson et al. 1996) perturbations were observed and consistent with theories of Alfvén wing model, but also have been discussed in the context of a unipolar inductor model (e.g., Goldreich and Lynden-Bell, 1969; Neubauer 1980; Goertz 1980; Gurnett & Goertz 1981; Bagenal 1983, Crary and Bagenal, 1997, Saur, 2004b). However, how these processes are coupled to Jupiter's ionosphere, which may be the primary place where the energy is dissipated, and how that energy is transferred to accelerating charged particles in the auroral region is still not well understood (e.g., Saur et al. 2004a, Kivelson et al. 2004, Clarke et al., 2004) due the lack of *in situ* measurements in the auroral regions during these epochs.

Recent analyses of the Juno magnetic field (Gershman et al., 2019), plasma wave (Sulaiman et al., 2020) and the low-energy charged particle data (Szalay et al., 2018, 2020a, 2020b) almost universally depict Alfvénic acceleration as a notable, if not dominant, electron acceleration mechanism associated with the IFP tail. More specifically, Gershman et al. (2019) found evidence of transverse magnetic field fluctuations consistent with strong magnetohydrodynamic (MHD) turbulence that can supply ~3,000 mW/m^2 of Alfvénic Poynting flux near Io's Main Alfvén Wing (MAW). Similarly, plasma wave observations presented by Sulaiman et al. (2020) show evidence of inertial Alfvén waves, intense ion cyclotron waves and whistler-mode auroral hiss radiation. Field-aligned low-energy (100 eV/Q to 100 keV/Q) electron beams with broadband energy distributions further support the existence of whistler-mode hiss and the imprints of stochastic particle acceleration via Alfvén waves (Szalay et al., 2018). Finally, a detailed look at the low-energy (10 eV/Q to 46 keV/Q) ion population suggests there is also a significant amount of proton acceleration occurring both at the high-latitudes (in similar locations to the electrons) and near the Io torus "boundary" – leading Szalay et al. (2020b) to hypothesize that Alfvén waves generated near Io may be an important acceleration mechanism for the protons as well.

In this work, we are motivated by the aforementioned studies (e.g., Gershman et al., 2019; Sulaiman et al., 2020, Szalay et al., 2020a, 2020b) to present the higher-energy charged particle observations with a particular focus on the proton data obtained during Juno's 12th perijove (PJ) crossing of the IFP tail in the northern hemisphere. We focus on the proton measurements because the Jupiter Energetic particle Detector Instrument (JEDI) (Mauk et al., 2017a) observed the most significant ion acceleration event to date, strongly suggesting that the electromagnetic coupling between Io and Jupiter is responsible for energizing protons up to ~ 1 MeV away from the planet. We compare these data to the magnetic field (Gershman et al., 2019) and plasma wave (Sulaiman et al., 2020) data from the same PJ12 IFP tail crossing near the MAW to better understand the underlying physics governing this unusually intense and unexpected event.

2. Observations

2.1 Juno's crossing of the IFP tail

The data presented here were collected on the inbound leg of PJ12 as Juno crossed the IFP tail in the northern hemisphere between ~09:20:35 to 09:20:55 UT on 2018-091 (01 April, 2018). Figure 1 is a trajectory schematic comprised of three different representations. Figure 1a illustrates Juno's intersection of a field line that maps to 5.9 Jovian radii (R_J, where 1 R_J =

71,492 km), i.e., Io's orbital position, in a cylindrical magnetic dipole coordinate system. Figure 1b is a northern polar projection of Jupiter's auroral regions in system III coordinates that encompasses the Io footprint tail (purple curve), Juno's magnetic footprint (orange curve) – calculated using the JRM09 model (Connerney et al., 2018), and the statistical position of the main auroral oval (black trace) derived from Hubble Space Telescope (HST) observations (e.g., Grodent et al., 2003). Juno crossed the IFP tail at an altitude of 0.39 R_J and with a longitudinal separation of approximately 1.7 degrees from Io's Main Alfvén Wing (MAW) spot (e.g., Bonfond et al., 2009) when account for the Alfvén wave trajectory bendback between Io and Jupiter's ionosphere. This remains Juno's closest approach to the MAW and potentially a direct crossing (Szalay et al., 2020a). Figure 1c shows Juno ultraviolet spectrometer (UVS) (Gladstone et al., 2017) observations of Jupiter's main auroral oval and the IFP tail approximately six minutes prior to Juno crossing Io's footprint tail. The UVS data are presented in a system III coordinate system with the red trace representing Juno's magnetic footprint.

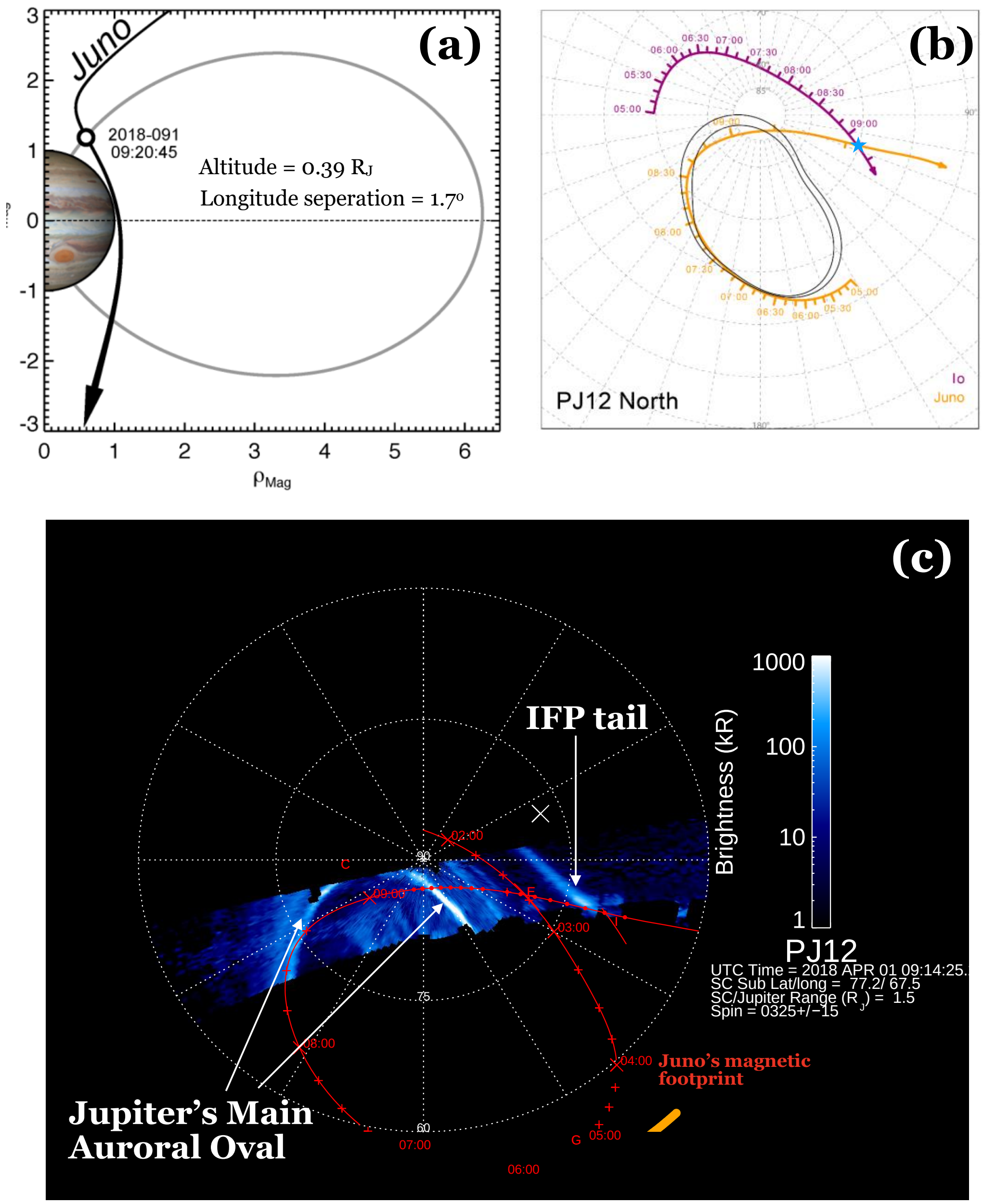

Figure 1: Io footprint tail crossing geometry. Panel a) Juno's trajectory in cylindrical magnetic coordinates with Io's M-Shell overlaid. Panel b) Magnetic footprints of Juno (orange curve), Io (purple) and the statistical location of Jupiter's main emission depicted by the bounding black curves (Bonfond et al., 2012). Panel c) Similar representation as panel b), but illustrates the ultraviolet brightness observations from Juno/UVS with Juno's magnetic footprint overlaid for reference (red curve). Juno/UVS observations occurred approximately six minutes before Juno crossed the IFP.

2.2 Brief description of Juno/JEDI

We focus on observations made by Juno's Jupiter Energetic particle Detector Instrument (JEDI). JEDI comprises three sensors (J90, J180 and J270) which measure the energy, angular and compositional distributions of >25 keV electrons and >10 keV ions (Mauk et al., 2017a). During this event, the J90 and J270 sensors operated in a high rate mode, thus accumulating time-of-flight by energy rates for 0.25 s at a cadence of 0.5 s, with no sector averaging. Pitch angle distributions were obtained by combining the JEDI measurements with the measured local magnetic field from Juno/MAG (Connerney et al., 2017b). The geometric loss cone size at this time is 40° based on the dipole field approximation and 51° based on the JRM09 magnetic field model (Connerney et al., 2018). Both methods agree well with the measured loss cone distributions in the ion data. Each solid-state telescope has a full width at half maximum field-of-view (FoV) that is approximately ~17° × 9° and therefore can resolve the loss cone in this region. The duration of the footprint tail crossing is ~20 seconds, which is shorter than it takes Juno to complete one revolution (Juno spins at ~2 revolutions per minute). This is important because instantaneous look directions and pitch angle averaging between the two sensors can average out fine structure in the IFP tail region. Therefore, we choose to perform all integral moment calculations, i.e., characteristic energies and energy fluxes, using a 1 second sampling window over a pitch angle range that contains just the upward moving protons (between 40° and 90°). The integral moment equations are outlined in Mauk et al. (2004) and Clark et al. (2018).

2.3 Energetic charged particle observations

Figure 2 presents an overview of the energetic charged particles (Fig. 2a – Fig. 2d) as well as the plasma wave electric field spectral densities (Fig. 2e) from Sulaiman et al. (2020) and the transverse magnetic field fluctuations (Fig. 2f) from Gershman et al. (2019). Plasma wave and magnetic field measurements were obtained from Juno's Waves (Kurth et al., 2017) and Magnetic field (Connerney et al., 2017b) investigations, respectively. The most prominent feature observed by JEDI is the dramatic proton intensity and pitch angle enhancements (Fig. 2c and 2d) corresponding to the IFP tail. In Fig. 2d, protons in the IFP tail are shown to be concentrated along the loss cone (horizontal dashed lines) in the upward direction. There is also evidence of ions streaming upward along the local magnetic field line, but that feature only persists for ~1 second. We do not discuss it further here. The energy-time distribution of the protons (Fig. 2c) reveal broad energization ranging from ~50 keV to upward of ~1 MeV. During the same time interval, the energetic electrons only show a modest response associated with the IFP tail. Figures 2a and 2b show a slight enhancement in low energy (< 60 keV) electrons and a slight decrease in the very energetic electron environment (>1 MeV), which leaves a signature indicated by the characteristic "penetrating charge particle" band near 160 keV (Mauk et al., 2018). While ions show significant intensities in the upward loss cone, electrons mostly populate the downward loss cone.

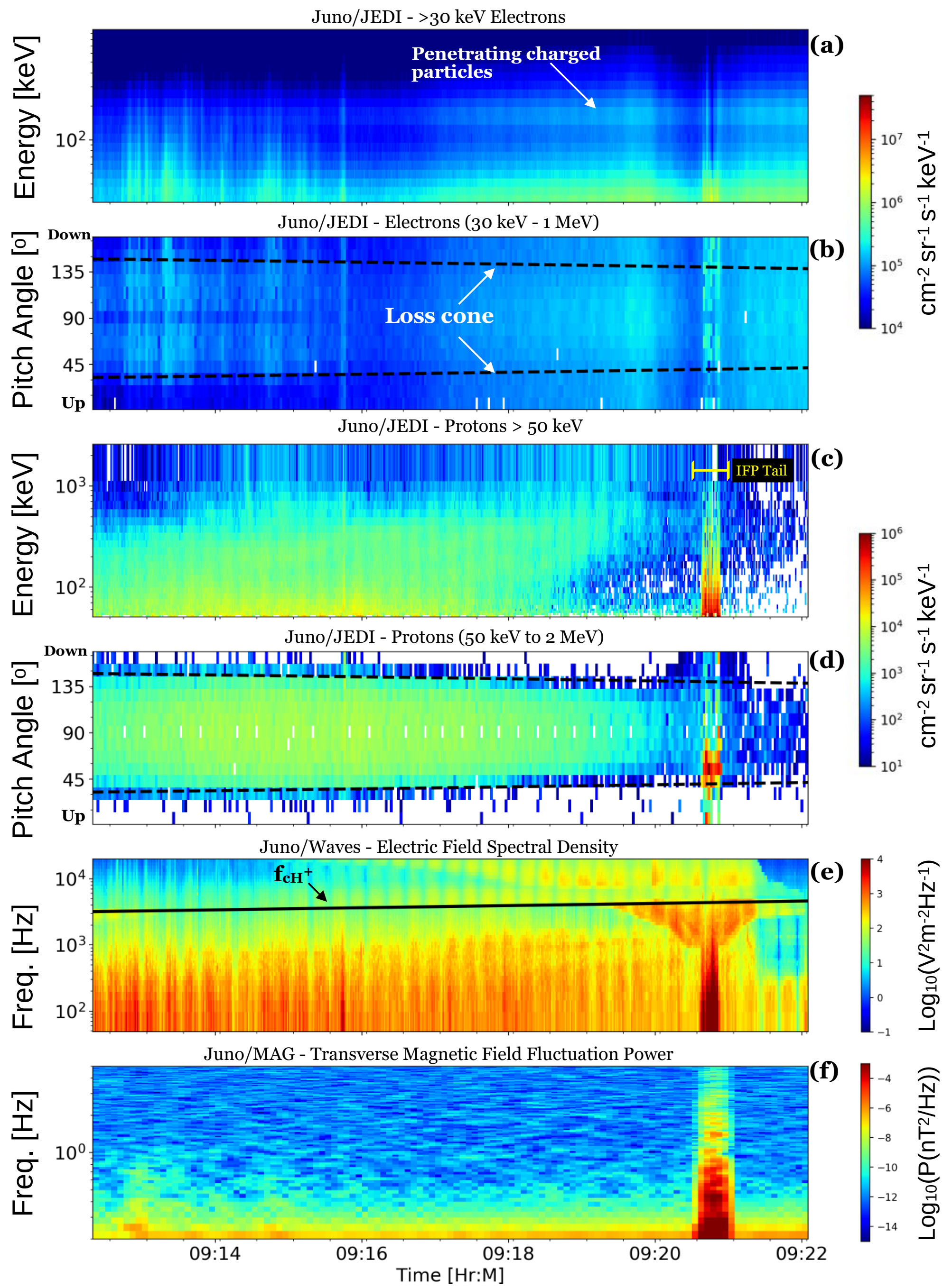

Figure 2: Particles and Fields overview of the Juno PJ12 IFP tail crossing. Panels a-d) illustrate the Juno/JEDI observations of the energetic electrons and protons. Panels a & b) energetic electron energy-time and pitch angle-time spectrograms, respectively. Panels c & d) energetic proton energy-time and pitch angle-time spectrograms, respectively. Panel e) electric field frequency-time spectrogram and panel f) magnetic field frequency-time spectrogram. The black dashed lines in panels c & d represent the size of the loss cone in degrees using the dipole field approximation. The black solid curve in panel e represents the proton cyclotron frequency derived by Juno/MAG (Sulaiman et al., 2020).

Figure 3 shows proton energy spectra and pitch angle distributions for various times associated with Io's footprint tail crossing. The energy distribution of the protons resemble a power-law – monotonically decreasing intensities toward increasing particle energy (see Fig. 3 left panel). There is no clear evidence of peaked or accelerated Maxwellian-like energy distributions, representative of magnetic field-aligned electric fields (Clark et al., 2017b, Mauk et al., 2017b; Mauk et al., 2018). In Fig. 3 the energy spectra from published Juno/JEDI proton observations are compared (Clark et al., 2017a, Mauk et al., 2018). The observations made in the footprint tail suggest that the protons are more efficiently accelerated than in the other auroral regions, which can be seen by the power-law curves representing $E^{-2.5}$ and $E^{-3.5}$. Pitch angle distributions for two different times show clear peaks with centroids near 53° and a full width at the 10% level of ~30°. Error bars in Figure 3 are determined by estimating the counting uncertainties associated with a Poisson distribution.

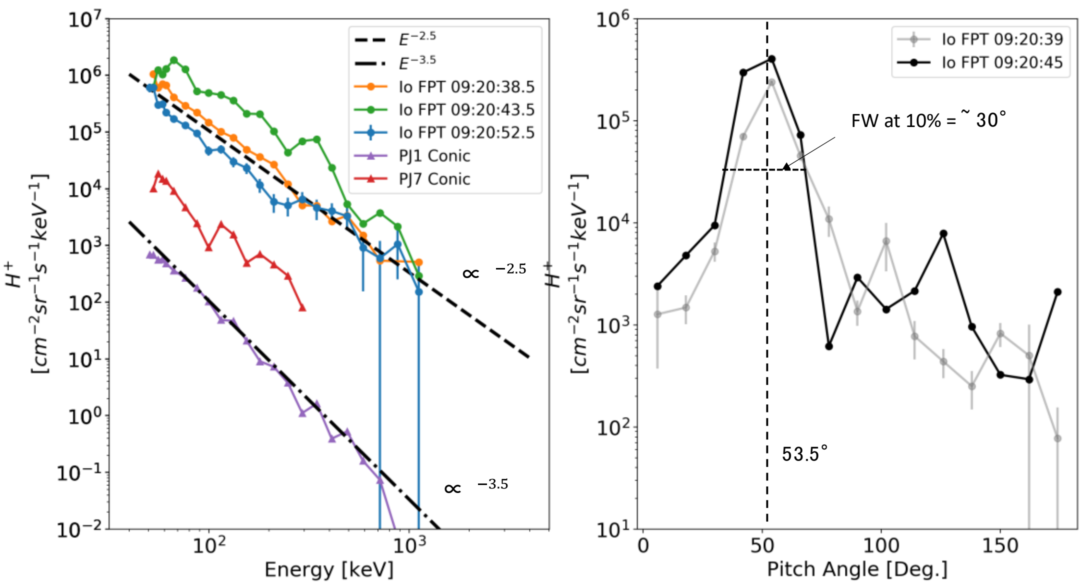

Figure 3: Measured energy spectra (left panel) and pitch angle distributions (right panel). For comparison purposes, energy spectra of proton conic distributions observed during PJ1 (Clark et al., 2017b) and PJ7 (Mauk et al., 2018) are also shown as well as power-law curves illustrating the different spectral slopes.

In Figure 4 we provide a closer inspection of the energy-time structuring and show the integral moments calculated using a one second sampling window over a pitch angle range that contains just the upward moving protons (between 40° and 90°). The energy-time spectrogram in Fig. 4a shows discrete stripes that occur somewhat regularly throughout the ~20 second IFP tail crossing. Similarly, in Fig. 4b the 100 keV proton intensities are chosen to highlight the variations, which fluctuate by factors of 3-10 on intervals as short as one second. Juno provides just a single point measurement and cannot disentangle the temporal/spatial ambiguity, therefore the 2-3 second variations may also be associated with ~50-100 km structures in the auroral region. It is possible that the variations are a measurement artifact due to the finite angular resolution of JEDI. A crude analysis suggests that a collimated beam of particles can produce a ~2 second variation in JEDI as a result of Juno's 12° s^{-1} rotation rate combined with the ~27° separation between the JEDI telescopes. This sort of temporal variation is observed in the polar cap where electron beams are often narrower than JEDI can resolve (Mauk et al., 2017a; Paranicas et al., 2018). In this particular event, the variation is likely not an artifact because the measured width of the proton pitch angle distribution is relatively broad, i.e., ~30° (see Fig. 3), compared to a single telescope FoV.

The integral moments associated with the IFP tail crossing show energetic protons characteristic energies varying between ~80 – 400 keV (with a mean ~200 keV) (Fig. 4c) and likewise the proton energy fluxes (Fig. 4d, averaged over pitch angles 40°-90° from ~50 keV to 1 MeV) to vary between ~10 mW/m^2 to ~100 mW/m^2 for the J90 sensor and ~1 mW/m^2 to ~30 mW/m^2 for the J270 sensor. Note that instantaneous pitch angle coverage is attributed to these differences. For comparison, we show the plasma electron (100 eV to 40 keV) precipitating energy fluxes (Szalay et al., 2020a) measured by Juno/JADE-E (McComas et al., 2017). JADE-E energy fluxes vary between ~3 - 600 mW/m^2.

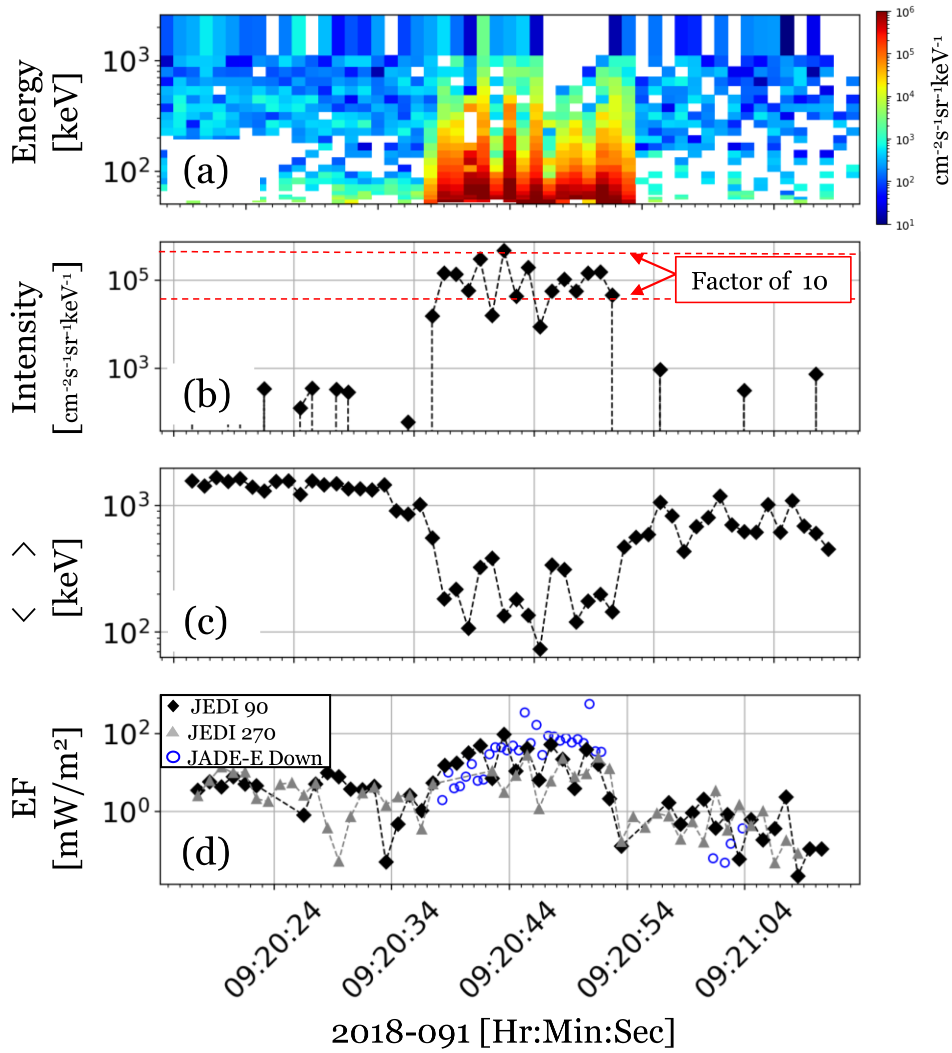

Figure 4: Panel a) JEDI J90 & 270 combined proton energy-time spectrogram filtered on pitch angles 40° - 90°; panel b) 100 keV proton intensities; panel c) > 50 keV proton characteristic energies; panel d) J90 (black diamonds), J270 (gray triangles) energetic proton energy flux vs. JADE-E (blue circles) energy fluxes of plasma electrons < 40 keV.

3. Discussion & Conclusions

The angular distribution of energetic protons along the upward loss cone reveal strong evidence for energetic ion conic acceleration associated with Io's footprint tail and probably the MAW. Ion conics are the result of thermal ionospheric ions heated perpendicular to the magnetic field via wave-particle interactions and then accelerated upward due to gradients in the magnetic field and/or field-aligned electric fields (e.g., Klumpar et al., 1979; Gorney et al., 1985; Chang, 1993;

Retterer et al., 1994; Carlson et al., 1998; Lynch et al., 2002). Wave-heating alone does not produce the most energetic ions; therefore, it is thought that electrostatic confinement via magnetic field-aligned potentials is required to trap the ions and further accelerate in the wave-heating region. This is referred to as the so-called "pressure cooker" mechanism (e.g., Gorney et al., 1985). Observations from Parker Solar Probe close to the Sun (Mitchell et al., 2020), Cassini at Saturn (Mitchell et al., 2009) and Juno at Jupiter (Clark et al., 2017b) have confirmed their existence elsewhere in the solar system, but have not been directly observed as a result of planet-moon interactions. Below we discuss possible proton acceleration mechanisms associated with the IFP tail.

The first mechanism we consider is a cyclotron resonant heating mechanism. Sulaiman et al. (2020) analyzed the Juno/Waves measurements during the PJ12 IFP tail crossing and found evidence of upward-propagating, left-hand polarized ion cyclotron waves with large spectral densities (maximum of ~10^5 $V^2m^{-2}Hz^{-1}$) near and at the proton cyclotron frequency. Using the theoretical energy transfer relationship from Chang et al. (1986), Sulaiman et al. (2020) estimated the ion heating rate, denoted as $dW_\perp/dt$, to have an upper limit of ~500 eV/s. To estimate the proton energies achievable from this heating rate we need to know the time-of-flight of the ions between their source region and the spacecraft. First, the altitude of the source region can be estimated from the measured pitch angle distributions, shown in Fig. 3, and by assuming the first adiabatic invariant is conserved as the protons are transported along the magnetic field. We also assume the protons are heated purely perpendicular to the local magnetic field, i.e., pitch angles of 90°, in the source region (see similar method outlined in Clark et al., 2017b and references therein) and neglect changes in an ion's pitch angle as it is transported along the field line. The measured local magnetic field during the IFP tail crossing is ~3×10^5 nT and the centroid of the proton pitch angle distributions vary between ~50° and 60°. Combining this information together and using the latest magnetic field model (JRM09; Connerney et al., 2018), we find the source location to be ~11,000 km or 0.16 R_J above Jupiter's 1-bar oblate surface. The last piece of information required is the bulk velocity of ions in Jupiter's ionosphere. The only published ion bulk flow measurements in this region to date is from a study of low-energy ions in Jupiter's topside ionosphere using the JADE-Ion sensor (Valek et al., 2020). The authors performed a numerical integration of the plasma proton distributions and derived an outflow speed, v_{bulk}, of 20 km/s. Here we assume this to be the outflow speed of the protons in the region connected to the IFP tail and thus, the time-of-flight of the protons is estimated to be approximately $t \approx 900$ s where, $t = d/v_{bulk}$, where $d = 18{,}500\ km$ is the integrated length along the field between Juno at $0.33\,R_J$ and the source region at $0.16\,R_J$. Multiplying the proton's time-of-flight with the heating rate derived by Sulaiman et al. (2020) suggests ion cyclotron heating may be able to produce conic energies as large as 450 keV. This number is commensurate with the characteristic energies of the proton observations in the IFP tail (see Fig. 4c). Major limitations of this crude estimate include the assumption that the wave-heating is constant along the flux tube between the source region and the spacecraft and the bulk ion speed remains the same. While the wave-heating assumption appears to be reasonable in Earth's auroral region (e.g., Lynch et al., 2002), it is uncertain if the same holds true for Jupiter. Next we consider the role of Alfvén waves as a possible energization mechanism.

Gershman et al. (2019) analyzed the magnetic field fluctuations in Jupiter's polar magnetosphere and found direct evidence of strong transverse perturbations associated with the IFP tail. The perturbations were identified as Alfvénic (between 0.2 to 5 Hz) and the Alfvén Poynting flux was calculated to be as high as ~3,000 mW/m^2 during the likely PJ12 crossing of Io's MAW. Sulaiman et al. (2020) used Juno/Waves data to demonstrate that Alfvénic fluctuations, first observed by MAG, extend into the higher frequencies spanning a range from ~50 to 800 Hz. Clearly, Alfvén waves are present and carry a significant source of energy in the IFP tail and near the MAW. In this letter, we do not address the fundamental idea regarding the role of Alfvén waves in generating ion conics, but we discuss important observational details and ideas that may help future theoretical pursuits. One striking observation is the energy partitioning between the Alfvénic Poynting flux and the particle energy fluxes. In Figure 4d, we show that the energetic ion energy flux is comparable to the 0.1 to 40 keV electron energy flux. If the energy reservoir is the same for the two populations then the observations presented here suggests that energy conversion efficiencies between Alfvén waves and ions (~3-5%) are comparable to the lower-energy electrons except for brief moments where the electron energy flux peaks as high as 580 mW/m^2. Numerous studies have investigated ion acceleration in Earth's aurorae and the role of Alfvén waves (e.g., Li and Temerin, 1993; Knudsen and Wahlund, 1998; Chaston et al., 2004). However, in the absence of wave-particle interaction models for the Io fluxtube and its tail, which consider the ion response specifically, we turn to comparisons with models at larger L-shells. Saur et al. (2018) find that on L-shells between 10 and 40 R_J, at high latitudes, ion-Landau damping is effectively not taking place, while electron Landau damping of inertial Alfvén waves is a highly effective acceleration mechanism in accordance with previous modeling and existing observations of energetic electrons (e.g. Hess et al. 2010, Hess et al. 2013, Bonfond et al. 2017, Saur et al. 2018, Clark et al., 2018, Szalay et al. 2020a). If the temporal scales of the waves become extremely small, then ion-cyclotron damping becomes more prominent (e.g., Sulaiman et al. 2020). Of the two resonant mechanisms discussed, i.e., Landau and cyclotron damping, non-resonant mechanisms (e.g., Lu and Li, 2007) of ion acceleration through Alfvén waves have not been studied for the Jupiter system and their effectiveness is thus difficult to assess without detailed studies.

The Juno/JEDI data presented in this study represent the first measurements of energetic proton conics associated with Io's footprint tail near the MAW. This discovery showcases the diversity of planetary systems and interactions present where ion conics exist, e.g., Earth, Saturn and Jupiter's auroral regions and now as a result of moon-magnetospheric interactions. Our primary conclusions in this study are the following:

1. Energetic proton acceleration associated with the IFP tail appears significant and perhaps the most intense ion event recorded by Juno/JEDI to date.

2. The angular distributions of the protons suggest these are the ion conic distributions and are likely accelerated by ion cyclotron waves via a resonant interaction; however, Alfvénic turbulence was not ruled out and may play a role.
3. Proton acceleration associated with Io's footprint tail is more intense than compared to the main auroral (Mauk et al., 2018) or polar cap regions (Clark et al., 2017b), thus highlighting the unique and strong electromagnetic interaction between Jupiter and Io.

Acknowledgements

The authors would like to thank Don Mitchell and Matina Gkioulidou for their discussions and assistance in understanding the corrected rates of the instrument. All Juno data presented here are publicly available from NASA's Planetary Data System as part of the JNO-J-JED-3_CDR-V1.0 data set for the Juno/JEDI instrument and The JNO-J/SW-JAD-3-CALIBRATED-V2.0 and JNO-J/SW-JAD-2-UNCALIBRATED-V1.0 for the Juno/JADE instrument. This work was supported by the Juno mission. The research at the University of Iowa was supported by NASA through Contract 699041X with the Southwest Research Institute.

References

Acuña, M. H., Neubauer, F. M., and Ness, N. F. (1981), Standing Alfvén wave current system at Io: Voyager 1 observations, *J. Geophys. Res.*, 86(A10), 8513– 8521, doi:10.1029/JA086iA10p08513.

Bagenal, F. (1983), Alfvén wave propagation in the Io plasma torus, *J. Geophys. Res.*, 88(A4), 3013– 3025, doi:10.1029/JA088iA04p03013.

Bagenal, F., Adriani, A., Allegrini, F., Bolton, S. J., Bonfond, B., Bunce, E. J., ... & Hansen, C. J. (2017). Magnetospheric science objectives of the Juno mission. *Space Science Reviews*, *213*(1-4), 219-287

Belcher, J. W., Goertz, C. K., Sullivan, J. D., and Acuña, M. H. (1981), Plasma observations of the Alfvén wave generated by Io, *J. Geophys. Res.*, 86(A10), 8508– 8512, doi:10.1029/JA086iA10p08508.

Bigg, E. K. (1964). Influence of the Satellite Io on Jupiter's Decametric Emission. *Nature*, *203*(4949), 1008–1010. https://doi.org/10.1038/2031008a0

Bonfond, B., Grodent, D., Gérard, J.-C., Radioti, A., Saur, J., and Jacobsen, S. (2008), UV Io footprint leading spot: A key feature for understanding the UV Io footprint multiplicity? *Geophys. Res. Lett.*, 35, L05107, doi:10.1029/2007GL032418.

Bonfond, B., Grodent, D., Gérard, J. C., Radioti, A., Dols, V., Delamere, P. A., & Clarke, J. T. (2009). The Io UV footprint: Location, inter-spot distances and tail vertical extent. *Journal of Geophysical Research: Space Physics*, *114*(A7).

Bonfond, B., Saur, J., Grodent, D., Badman, S. V., Bisikalo, D., Shematovich, V., ... & Radioti, A. (2017). The tails of the satellite auroral footprints at Jupiter. *Journal of Geophysical Research: Space Physics*, *122*(8), 7985-7996

Carlson, C. W., McFadden, J. P., Ergun, R. E., Temerin, M., Peria, W., Mozer, F. S., … Pfaff, R. (1998). FAST observations in the downward auroral current region: Energetic upgoing electron beams, parallel potential drops, and ion heating. *Geophysical Research Letters*, *25*(12), 2017–2020. https://doi.org/10.1029/98GL00851

Chaston, C. C., Bonnell, J. W., Carlson, C. W., McFadden, J. P., Ergun, R. E., Strangeway, R. J., & Lund, E. J. (2004). Auroral ion acceleration in dispersive Alfvén waves. *Journal of Geophysical Research: Space Physics*, *109*(A4).

Chang, T., Crew, G. B., Hershkowitz, N., Jasperse, J. R., Retterer, J. M., & Winningham, J. D. (1986). Transverse acceleration of oxygen ions by electromagnetic ion cyclotron resonance with broad band left-hand polarized waves. *Geophysical Research Letters*, *13*(7), 636-639.

Clark, G., et al. (2017b), Observation and interpretation of energetic ion conics in Jupiter's polar magnetosphere, *Geophys. Res. Lett.*, 44, 4419– 4425, doi:10.1002/2016GL072325.

Clark, G., et al. (2017a), Energetic particle signatures of magnetic field-aligned potentials over Jupiter's polar regions, *Geophys. Res. Lett.*, 44, 8703– 8711, doi:10.1002/2017GL074366.

Clark, G., Tao, C., Mauk, B. H., Nichols, J., Saur, J., Bunce, E. J., et al. (2018). Precipitating electron energy flux and characteristic energies in Jupiter's main auroral region as measured by Juno/JEDI. *Journal of Geophysical Research: Space Physics*, 123, 7554– 7567. https://doi.org/10.1029/2018JA025639

Clarke, J. T., Ballester, G. E., Trauger, J., Evans, R., Connerney, J. E. P., Stapelfeldt, K., … Westphal, J. A. (1996). Far-Ultraviolet Imaging of Jupiter’s Aurora and the Io “Footprint.” *Science*, *274*(5286), 404 LP-409. https://doi.org/10.1126/science.274.5286.404

Chang, T. (1993). Lower-hybrid collapse, caviton turbulence, and charged particle energization in the topside auroral ionosphere and magnetosphere*. *Physics of Fluids B: Plasma Physics*, *5*(7), 2646–2656. https://doi.org/10.1063/1.860702

Connerney, J. E. P., Baron, R., Satoh, T., & Owen, T. (1993). Images of Excited H3+ at the Foot of the lo Flux Tube in Jupiter’s Atmosphere. *Science*, *262*(5136), 1035 LP-1038. https://doi.org/10.1126/science.262.5136.1035

Connerney, J. E. P., Adriani, A., Allegrini, F., Bagenal, F., Bolton, S. J., Bonfond, B., … Waite, J. (2017a). Jupiter’s magnetosphere and aurorae observed by the Juno spacecraft during its first polar orbits. *Science*, *356*(6340), 826 LP – 832. https://doi.org/10.1126/science.aam5928

Connerney, J. E. P., Benn, M., Bjarno, J. B., Denver, T., Espley, J., Jorgensen, J. L., … Smith, E. J. (2017b). The Juno Magnetic Field Investigation. *Space Science Reviews*, *213*(1), 39–138. https://doi.org/10.1007/s11214-017-0334-z

Connerney, J. E. P., Kotsiaros, S., Oliversen, R. J., Espley, J. R., Jørgensen, J. L., Joergensen, P. S., ... & Bolton, S. J. (2018). A new model of Jupiter's magnetic field from Juno's first nine orbits. *Geophysical Research Letters*, *45*(6), 2590-2596.

Crary, F. J., & Bagenal, F. (1997). Coupling the plasma interaction at Io to Jupiter. *Geophysical Research Letters*, *24*(17), 2135–2138. https://doi.org/10.1029/97GL02248

Frank, L. A., Paterson, W. R., Ackerson, K. L., Vasyliunas, V. M., Coroniti, F. V, & Bolton, S. J. (1996). Plasma Observations at Io with the Galileo Spacecraft. *Science*, *274*(5286), 394 LP – 395. https://doi.org/10.1126/science.274.5286.394

Gerard, J.-C., A. Saglam, D. Grodent, and J. T. Clarke (2006), Morphologyof the ultraviolet emission and its control by Io's location,J. Geophys.Res.,111, A04202, doi:10.1029/2005JA011327.

Gershman, D. J., Connerney, J. E. P., Kotsiaros, S., DiBraccio, G. A., Martos, Y. M., F.-Viñas, A., et al. (2019). Alfvénic fluctuations associated with Jupiter's auroral emissions. *Geophysical Research Letters*, 46,7157– 7165. https://doi.org/10.1029/2019GL082951

Gladstone, G. R., Persyn, S. C., Eterno, J. S., Walther, B. C., Slater, D. C., Davis, M. W., ... & Sawka, A. O. (2017). The ultraviolet spectrograph on NASA's Juno mission. *Space Science Reviews*, *213*(1-4), 447-473.

Goertz, C. (1980), Io's interaction with the plasma torus, *J. Geophys. Res.*, 85(A6), 2949– 2956, doi:10.1029/JA085iA06p02949.Kivelson, M. G., Khurana, K. K., Walker, R. J., Russell, C. T., Linker, J. A., Southwood, D. J., & Polanskey, C. (1996). A Magnetic Signature at Io: Initial Report from the Galileo Magnetometer. *Science*, *273*(5273), 337 LP – 340. https://doi.org/10.1126/science.273.5273.337

Goldreich, P., & Lynden-Bell, D. (1969). Io, a Jovian unipolar inductor. *The Astrophysical Journal*, *156*, 59-78.

Gorney, D. J., Chiu, Y. T., & Croley Jr, D. R. (1985). Trapping of ion conics by downward parallel electric fields. *Journal of Geophysical Research: Space Physics*, *90*(A5), 4205-4210.

Grodent, D., Clarke, J. T., Kim, J., Waite Jr, J. H., & Cowley, S. W. H. (2003). Jupiter's main auroral oval observed with HST-STIS. *Journal of Geophysical Research: Space Physics*, *108*(A11).

Gurnett, D. A., and Goertz, C. K. (1981), Multiple Alfven wave reflections excited by Io: Origin of the Jovian decametric arcs, *J. Geophys. Res.*, 86(A2), 717– 722, doi:10.1029/JA086iA02p00717.

Gurnett, D. A., Kurth, W. S., Roux, A., Bolton, S. J., & Kennel, C. F. (1996). Galileo Plasma Wave Observations in the Io Plasma Torus and Near Io. *Science*, *274*(5286), 391 LP – 392. https://doi.org/10.1126/science.274.5286.391

Hess, S. L., Delamere, P., Dols, V., Bonfond, B., & Swift, D. (2010). Power transmission and particle acceleration along the Io flux tube. *Journal of Geophysical Research: Space Physics*, *115*(A6).

Hess, S. L. G., Bonfond, B., Chantry, V., Gérard, J. C., Grodent, D., Jacobsen, S., & Radioti, A. (2013). Evolution of the Io footprint brightness II: Modeling. *Planetary and Space Science*, *88*, 76-85.

Kivelson, M. G., Khurana, K. K., Walker, R. J., Russell, C. T., Linker, J. A., Southwood, D. J., & Polanskey, C. (1996). A magnetic signature at Io: Initial report from the Galileo magnetometer. *Science*, *273*(5273), 337-340.

Klumpar, D. M. (1979), Transversely accelerated ions: An ionospheric source of hot magnetospheric ions, *J. Geophys. Res.*, 84(A8), 4229– 4237, doi:10.1029/JA084iA08p04229.

Knudsen, D. J., & Wahlund, J. E. (1998). Core ion flux bursts within solitary kinetic Alfvén waves. *Journal of Geophysical Research: Space Physics*, *103*(A3), 4157-4169.

Kurth, W. S., Hospodarsky, G. B., Kirchner, D. L., Mokrzycki, B. T., Averkamp, T. F., Robison, W. T., … Zarka, P. (2017). The Juno Waves Investigation. *Space Science Reviews*, *213*(1), 347–392. https://doi.org/10.1007/s11214-017-0396-y

Li, X., & Temerin, M. (1993). Ponderomotive effects on ion acceleration in the auroral zone. *Geophysical research letters*, *20*(1), 13-16.

Lu, Q., & Li, X. (2007). Heating of ions by low-frequency Alfven waves. *Physics of Plasmas*, *14*(4), 42303. https://doi.org/10.1063/1.2715569

Lynch, K. A., Bonnell, J. W., Carlson, C. W., and Peria, W. J., Return current region aurora: $E_{\parallel}$, j_z, particle energization, and broadband ELF wave activity, *J. Geophys. Res.*, 107(A7), doi:10.1029/2001JA900134,2002.

Mitchell, D. G., Kurth, W. S., Hospodarsky, G. B., Krupp, N., Saur, J., Mauk, B. H., Carbary, J. F., Krimigis, S. M., Dougherty, M. K., and Hamilton, D. C. (2009), Ion conics and electron beams associated with auroral processes on Saturn, *J. Geophys. Res.*, 114, A02212, doi:10.1029/2008JA013621.

Mitchell, D. G., Giacalone, J., Allen, R. C., Hill, M. E., McNutt, R. L., McComas, D. J., et al. (2020). CME-associated Energetic Ions at 0.23 au: Consideration of the Auroral Pressure Cooker Mechanism Operating in the Low Corona as a Possible Energization Process. *The Astrophysical Journal Supplement Series*, *246*(2), 0–0. http://doi.org/10.3847/1538-4365/ab63cc

Mauk, B. H., Mitchell, D. G., McEntire, R. W., Paranicas, C. P., Roelof, E. C., Williams, D. J., … Lagg, A. (2004). Energetic ion characteristics and neutral gas interactions in Jupiter's magnetosphere. *Journal of Geophysical Research: Space Physics*, *109*(A9). https://doi.org/10.1029/2003JA010270

Mauk, B. H., Haggerty, D. K., Jaskulek, S. E., Schlemm, C. E., Brown, L. E., Cooper, S. A., … Stokes, M. R. (2017a). The Jupiter Energetic Particle Detector Instrument (JEDI) Investigation for the Juno Mission. *Space Science Reviews*, *213*(1), 289–346. https://doi.org/10.1007/s11214-013-0025-3

Mauk, B. H., Haggerty, D. K., Paranicas, C., Clark, G., Kollmann, P., Rymer, A. M., … Valek, P. (2017b). Discrete and broadband electron acceleration in Jupiter's powerful aurora. *Nature*, *549*(7670), 66–69. https://doi.org/10.1038/nature23648

Mauk, B. H., Haggerty, D. K., Paranicas, C. P., Clark, G., Kollmann, P., Rymer, A. M., … Valek, P. (2018). Diverse electron and ion acceleration characteristics observed over Jupiter's main aurora. *Geophysical Research Letters*, 1277–1285. https://doi.org/10.1002/2017GL076901

McComas, D. J., Alexander, N., Allegrini, F., Bagenal, F., Beebe, C., Clark, G., … White, D. (2017). The Jovian Auroral Distributions Experiment (JADE) on the Juno Mission to Jupiter. *Space Science Reviews*, *213*(1), 547–643. https://doi.org/10.1007/s11214-013-9990-9

Neubauer, F. (1980), Nonlinear standing Alfvén wave current system at Io: Theory, *J. Geophys. Res.*, 85(A3), 1171– 1178, doi:10.1029/JA085iA03p01171.

Paranicas, C., Mauk, B. H., Haggerty, D. K., Clark, G., Kollmann, P., Rymer, A. M., et al. (2018). Intervals of intense energetic electron beams over Jupiter's poles. *Journal of Geophysical Research: Space Physics*, 123, 1989– 1999. https://doi.org/10.1002/2017JA025106

Queinnec, J., & Zarka, P. (1998). Io-controlled decameter arcs and Io-Jupiter interaction. *Journal of Geophysical Research: Space Physics*, *103*(A11), 26649-26666.

Retterer, J. M., Chang, T., and Jasperse, J. R. (1994), Transversely accelerated ions in the topside ionosphere, *J. Geophys. Res.*, 99(A7), 13189– 13201, doi:10.1029/93JA03570.

Saur, J., F. M. Neubauer, J. E. P. Connerney, P. Zarka, and M. G. Kivelson (2004a), Plasma interaction of Io with its plasma torus, in Jupiter: The Planet, Satellites and Magnetosphere, edited by F. Bagenal, T. Dowling, and W. McKinnon, pp. 537–560, Cambridge Univ. Press, New York.

Saur, J. (2004b), A model of Io's local electric field for a combined Alfvénic and unipolar inductor far-field coupling, *J. Geophys. Res.*, 109, A01210, doi:10.1029/2002JA009354.

Saur, J., Grambusch, T., Duling, S., Neubauer, F. M., & Simon, S. (2013). Magnetic energy fluxes in sub-Alfvénic planet star and moon planet interactions. *A&A, 552, A119*. Retrieved from https://doi.org/10.1051/0004-6361/201118179

Saur, J., Janser, S., Schreiner, A., Clark, G., Mauk, B. H., P., Kollmann, et al. (2018). Wave-particle interaction of Alfvén waves in Jupiter's magnetosphere: Auroral and magnetospheric particle acceleration. *Journal of Geophysical Research: Space Physics*, 123, 9560– 9573. https://doi.org/10.1029/2018JA025948

Sulaiman, A. H., Hospodarsky, G. B., Elliott, S. S., Kurth, W. S., Gurnett, D. A., Imai, M., ... & Ebert, R. W. (2020). Wave-particle interactions associated with Io's auroral footprint: Evidence of Alfvén, ion cyclotron, and whistler modes. *Geophysical Research Letters*, e2020GL088432.

Szalay, J. R., Bonfond, B., Allegrini, F., Bagenal, F., Bolton, S., Clark, G., et al. (2018). In situ observations connected to the Io footprint tail aurora. *Journal of Geophysical Research: Planets*, 123, 3061– 3077. https://doi.org/10.1029/2018JE005752

Szalay, J. R., et al. (2020a, in press), A new framework to explain changes in Io's footprint tail electron fluxes, *GRL*

Szalay, J. R. et al. (2020b), Proton Acceleration by Io's Alfvénic Interaction, *Journal of Geophysical Research: Space Physics*, 124. https://doi.org/10.1029/2019JA027314

Valek, P. W., Bagenal, F., Ebert, R. W., Allegrini, F., McComas, D. J., Szalay, J. R., ... & Connerney, J. E. P. (2020). Juno in situ observations above the Jovian equatorial ionosphere. *Geophysical Research Letters*, *47*(12), e2020GL087623.

Williams, D. J., Mauk, B. H., McEntire, R. E., Roelof, E. C., Armstrong, T. P., Wilken, B., … Lanzerotti, L. J. (1996). Electron Beams and Ion Composition Measured at Io and in Its Torus. *Science*, *274*(5286), 401 LP – 403. https://doi.org/10.1126/science.274.5286.401

Zarka, P. (2000). Radio emissions from the planets and their moons. *GEOPHYSICAL MONOGRAPH-AMERICAN GEOPHYSICAL UNION*, *119*, 167-178.

530